

Influence of Explosion Interval on the Acoustic Characteristics of Underwater Continuous Explosion

DZ Zhao², XM Chen¹, DN Gu¹, Q Ma², CA Guo¹, S Zhao^{1*}

1. Shenyang Ligong University, Shenyang 110159, China

2. Huaan Industry Group Co., Ltd., Qiqihar 161046, China

ABSTRACT

In this paper, the acoustic signal of the underwater explosion was taken as the main research object, and the mechanical and acoustic characteristics of the underwater explosion were studied by combining theoretical research with simulation, the propagation law of shock wave and the acoustic characteristics of explosion signal with different explosion depth and charge were obtained. The results show that the underwater explosion has strong acoustic power, high sound pressure level, wide frequency coverage of explosion acoustic signal. In low frequency band, the acoustic power level decays rapidly with the increase of frequency, and its acoustic energy is very high; in higher frequency band, the acoustic power level decays slowly, and its sound energy is relatively low; bubble pulsation has a great influence on the energy distribution of acoustic power level, and the more bubble pulsation times, the greater the proportion of low-frequency energy. The research results of this article can provide a theoretical basis for the research of fuze anti-interference.

1. INTRODUCTION

With the increasing demand of marine development and military, higher requirements are put forward for high-precision underwater target detection technology. In the process of underwater targets detection, underwater explosion is the simplest and most effective interference source [1]. When explosives explode underwater, they will produce strong shock waves, which will quickly decay into underwater acoustic waves and form interference noise with high acoustic source level. Underwater continuous explosion not only has the characteristics of underwater explosion, but also can effectively prolong the interference time on the basis of single explosion. The continuous explosion signal has a wide frequency band, almost covering all working frequencies of the mine fuze, which brings great challenges to the detection, identification, and positioning of the target of the mine fuze, and has become an important interference technical means against sonar detection in various countries [2].

At present, the research on underwater explosion is mainly divided into three methods: theoretical analysis, experimental studies, and numerical simulation. Theoretical analysis mainly studies the structural response of simple rules. Experimental research can be destructive, and few underwater explosion experiments have been made public. Therefore, the study of underwater explosion through simulation has become the main means, such as LS-DYNA, DYTRAN, ABAQUS, AUTODYN, etc., which can comprehensively analyze the related problems of underwater explosion.

*Corresponding Author: 544383414@qq.com

Sun et al. [3] summarized the empirical formula of ultra near field underwater explosion shock wave and the peak value change law of aluminized explosives underwater explosion shock wave, which has certain reference value for predicting the near field shock wave pressure. Ma et al. [4] carried out the scaling experiment of centrifuge underwater explosion, which solved the problems that the traditional scaling experiment could not scale the water depth and the bubble pulsation error was large and provided a new idea for the research of underwater explosion. Liu et al. [5] simulated spherical explosives based on centrifuge underwater explosion test. It is concluded that with the increase of explosion depth, the peak pressure of shock wave at the same monitoring point increases, but the increase range is small. Meng et al. [6] used AUTODYN simulation software to numerically simulate small equivalent TNT charges, obtaining the influence of different explosion depths on bubble pulsation, and summarized the relationship between bubble pulsation period and bubble expansion radius with explosion depth.

Underwater explosion shock wave will decay continuously in the process of propagating outward, and they will decay into acoustic signals after propagating a certain distance. The analysis methods of underwater explosion pressure signals mainly include Fourier transform, short-time Fourier transform, wavelet transform, wavelet packet transform, Hilbert-Huang transform, etc. [7-11]. Weston [12] used Fourier transform to process the shock wave and bubble pulse semi-empirical formula fitted by Arons [13-14] and projected the time domain relationship into the frequency domain to obtain the energy flow density spectrum and analyzed the influence of explosive mass and explosion depth on the energy flow density spectrum. Liu et al. [15] proposed an algorithm to mark and intercept the direct acoustic component of underwater explosion and analyzed the spectral characteristics of the captured fragments combined with underwater explosion experiments in shallow water. Wu et al. [16] obtained underwater explosion acoustic signals through experiments, conducted time-frequency analysis on them, obtained the acoustic characteristics of underwater explosion acoustic signals, determined, and verified the role played by underwater explosion acoustic signals in hydroacoustic interference countermeasures. Fan et al. [17] extracted and analyzed the underwater explosion acoustic signals by wavelet analysis, studied the frequency and distribution characteristics of the signals and obtained the acoustic characteristics of the underwater explosion acoustic signals. Sheng [18] decomposed the explosion acoustic signals by wavelet transform and HHT, calculated the power spectrum, energy distribution, Hilbert spectrum, and marginal spectrum of the signals, and studied the influence of detonation interval time on the continuous explosion acoustic signals.

In summary, many scholars focus on the propagation process of underwater explosion, shock wave characteristics, and damage effects. However, there are few reports on the shock wave propagation of underwater explosion with different depth, different charge, and different explosion interval. The study on acoustic characteristics of continuous underwater explosion is still not complete. Therefore, this paper took underwater continuous explosion as the main research object, used AUTODYN simulation software for numerical simulation to obtain the mechanical and acoustic characteristics of underwater explosions with different parameters under different explosion depths, different charge quantities, and different explosion intervals. It is expected that the characteristics of underwater explosion interference sources can be deeply understood, which provides a theoretical basis for the research of fuze anti-interference.

2. BASIC PRINCIPLE OF UNDERWATER EXPLOSION

The explosion process is divided into three stages: charge detonation, shock wave shock wave propagation, and bubble pulsation [15]. Explosives release a large amount of energy during the detonation stage, forming high-temperature and high-pressure detonation products. Subsequently, an outward propagating shock wave is formed in the water, which can be attenuated to water acoustic waves at a certain distance. When the initial shock wave is formed, the detonation products expand outward rapidly and push the surrounding water to move outward along the radial direction in the form of bubbles, and bubble pulsation is formed through repeated expansion and contraction. Shock wave and bubble pulsation show different physical characteristics, and the peak pressure of shock wave is large, but the duration is short; the peak pressure of bubble pulsation is small, and the duration is long. The acoustic signal generated by an underwater explosion is shown in Figure 1.

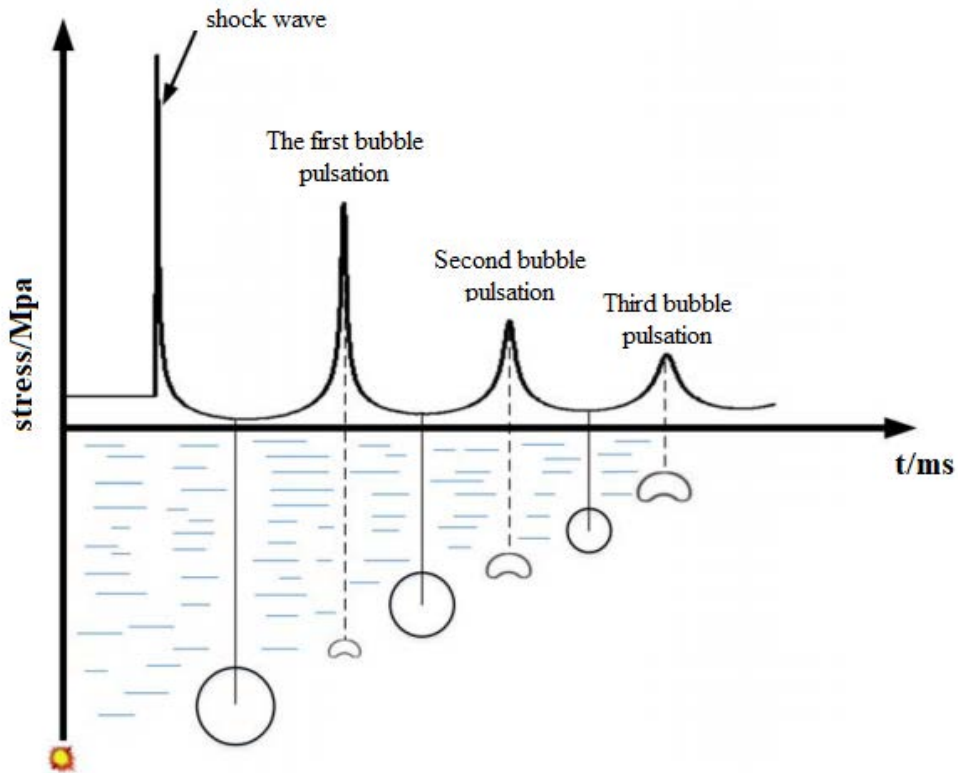


Fig.1. Schematic diagram of underwater explosion acoustic signal structure and generation process

3. NUMERICAL CALCULATION OF UNDERWATER EXPLOSION OF SPHERICAL TNT CHARGE

3.1. Underwater Single Explosion Simulation

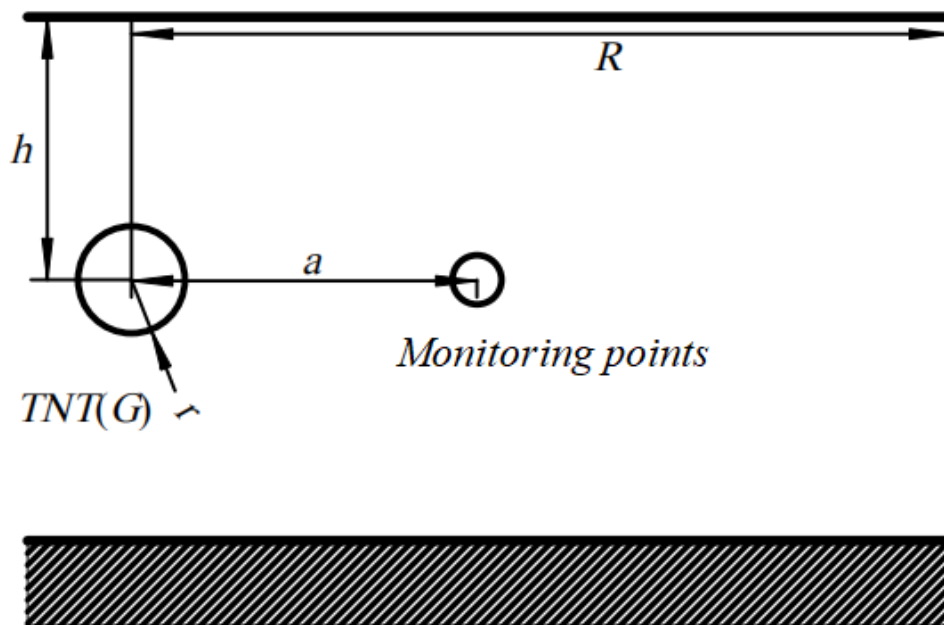


Fig.2. Underwater explosion model

Figure 2. shows the underwater explosion model, in which the TNT charge mass is G , the charge radius is r , the charge explosion depth is h , the water area radius is R , and the distance between the monitoring point and the TNT charge is a .

According to Figure 2., a one-dimensional axisymmetric calculation model is established, assuming that a spherical naked explosive explodes in infinite water, using wedge elements. The model consists of water medium and TNT, where the mass G of TNT spherical explosive is 1 kg, the charge radius r is 55 mm, and the initiation method is center initiation. The radius R of the calculated model water area is 300 meters, and the TNT explosion depth h is taken as 30 meters, 50 meters, 70 meters, 100 meters, 150 meters, and 200 meters, respectively. The distance a between the monitoring point and the TNT charge is from 1 meter to 50 meters, and the boundary is set as the outflow boundary. The water medium and TNT are both Euler grids. In order to ensure the calculation accuracy and improve the computational efficiency, the division method of local encrypted grids is adopted. Each grid at a distance of 1m from the explosion center is set at 1 mm with a total of 60800 grids. TNT charges are filled in the water area, as shown in Figure 3.

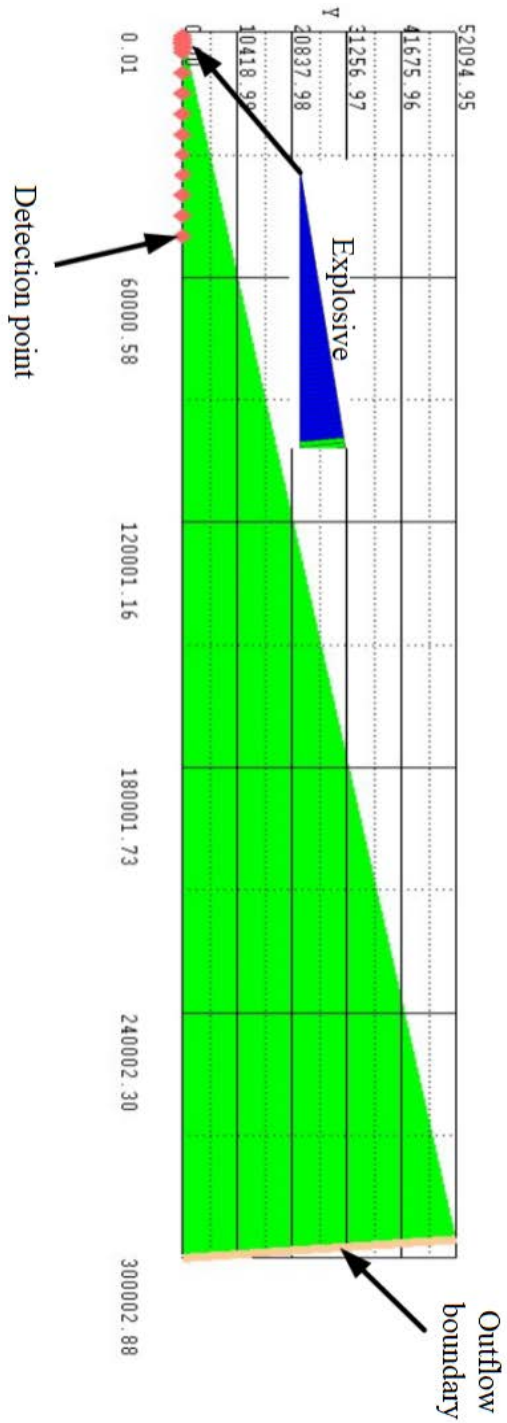


Fig.3. Simulation calculation model

The TNT explosive state equation adopts the JWL state equation as follows:

$$P = A\left(1 - \frac{\omega\eta}{R_1}\right)e^{-\frac{R_1}{\eta}} + B\left(1 - \frac{\omega\eta}{R_2}\right)e^{-\frac{R_2}{\eta}} + \omega\eta\rho_0 e \quad (1)$$

where in the equation, $\eta = \rho/\rho_0$; A , B , ω , R_1 and R_2 are constants, with values shown in Table 1.

Table 1. Main parameters of TNT explosives

A (GPa)	B (GPa)	R₁	R₂	ω	ν (m·s ⁻¹)	ρ (g·cm ⁻³)	Q_v (kJ·kg ⁻¹)
371.2	3.231	4.15	0.95	0.3	6930	1630	4294

At present, many scholars adopt the Mie-Gruneisen state equation for underwater explosion, but Liu Kezhong et al. believe that the error between the polynomial state equation of AUTODYN software and the empirical formula is smaller in the process of shallow water explosion, and the numerical simulation is relatively more accurate. Therefore, the polynomial equation is used to calculate the water medium in this paper. When $\mu > 0$, it is in a compressed state; when $\mu < 0$, it is in a stretched state. The specific form is:

$$\begin{cases} p = A_1\mu + A_2\mu^2 + A_3\mu^3 + (B_0 + B_1\mu)\rho_0 E_M \\ p = T_1\mu + T_2\mu^2 + B_0\rho_0 E_M \end{cases} \quad (2)$$

where in the formula, p is the pressure of the water medium; $\rho_0 = 1.0 \text{ g/cm}^3$; $\mu + 1 = \frac{\rho}{\rho_0}$, where ρ is the density of the water medium; $A_1, A_2, A_3, T_1, T_2, B_0, B_1$ are constants; E_M is the specific internal energy of the water medium.

$$E_M = \frac{p_0 + \rho_0 gH}{B_0} \quad (3)$$

where in the equation, p_0 is atmospheric pressure, taken as $1.013 \times 10^5 \text{ Pa}$; g is the gravitational acceleration, taken as 9.8 g/cm^3 ; H is the water depth.

The parameter settings for the water state equation are shown in Table 2.

Table 2. Polynomial state equation parameters of water provided

A₁ (GPa)	A₂ (GPa)	A₃ (GPa)	B₀	B₁	T₁ (GPa)	T₂ (GPa)
2.2	9.54	14.57	0.28	0.28	2.2	0

There will be sudden changes in pressure and density before and after the shock wave array of the underwater explosion, which makes it difficult to solve the differential equation. The artificial viscosity coefficient is usually introduced in calculations to solve this problem. The

artificial viscosity coefficient in the AUTODYN program is:

$$q = \begin{cases} \rho'(C_L l c \varepsilon + C_Q^2 l^2 \varepsilon^2) & , \varepsilon < 0 \\ 0 & , \varepsilon \geq 0 \end{cases} \quad (4)$$

where C_L is the artificial viscosity coefficient of the first order term; C_Q is the quadratic term artificial viscosity coefficient; l is the feature-length; ρ is the material density; c is the velocity of sound in the material; ε is the rate of change in volume. In order to improve the accuracy of simulation calculations, $C_Q = 0.1$ was selected, the C_L value was changed, and the error size was compared to determine the artificial viscosity coefficient in this paper.

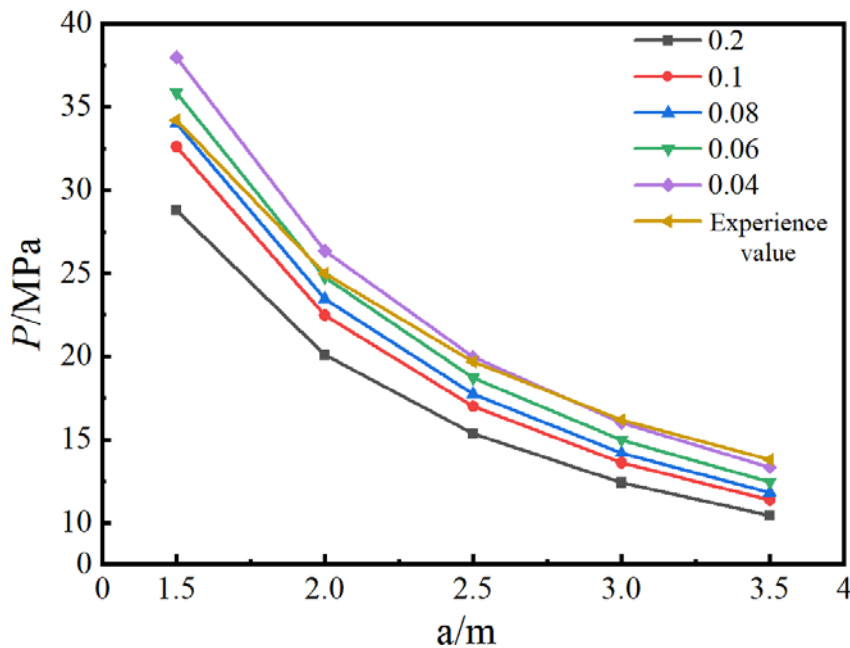


Fig. 4. Variation of peak pressure of shock wave with distance from explosive under different C_L

Figure 4. shows the variation curves of the peak pressure of shock wave with the distance from the explosive position under different C_L . As shown in Figure 4, C_L has a significant influence on the peak pressure of the shock wave. With the decrease of CL, the peak pressure of shock wave shows an increasing trend. When C_L is less than 0.06, it is found that the relative error is less than 10% by comparing with the empirical formula, which indicates that the accuracy of numerical simulation can be improved by taking a smaller C_L value in numerical simulation calculations. Therefore, it is determined that the C_L of the numerical simulation in this paper is 0.06.

Figure 5. shows the time history curves of underwater explosion shock wave pressure at the explosion distance of 1 m~4 m. It can be seen from Figure 5. that the shock wave generated by the underwater explosion instantly increases to the peak pressure. With the increase of time, the peak pressure of the shock wave decays exponentially, and the peak pressure of the shock wave decreases with the increase of the explosion distance.

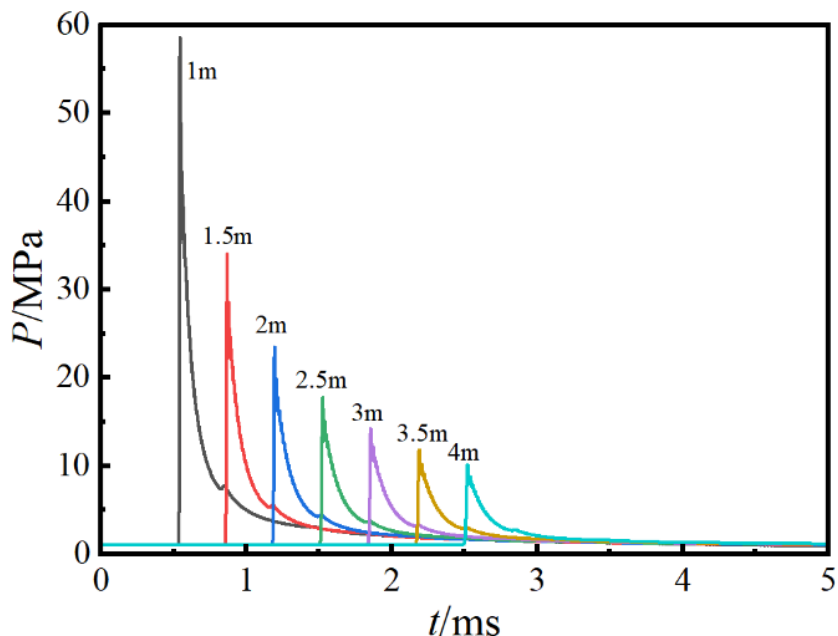


Fig. 5. Pressure curves of underwater explosion shock wave with detonation distance of 1 m~4 m

Figure 6 shows the comparison between empirical values and simulation calculations of peak pressure at different ratios of detonation distance. By the analysis of Figure 6, it can be seen that the numerical simulation results of the peak pressure of the shock wave in the mid-to-far field are consistent with the analytical results of the empirical formula. The maximum absolute error of numerical simulation results is 8%, which occurs at a distance of 20 times the explosion proportion. In summary, the numerical simulation results are consistent with the empirical formula, and the error between them is less than 10%. It can be considered that the numerical simulation model has a certain degree of reliability and rationality. After analysis, there are two reasons for the error between the numerical simulation model and the empirical formula. On one hand, the shock wave in the numerical calculation is a strong discontinuity, and artificial viscosity is needed to solve the non-material understanding caused by the strong discontinuity in the solution. Therefore, there are certain errors in the numerical solution; on the other hand, because there is no energy loss caused by the work of bubbles floating upward when calculating the underwater explosion problem with a one-dimensional wedge grid, the theoretical numerical solution results are greater than the empirical formula solution results.

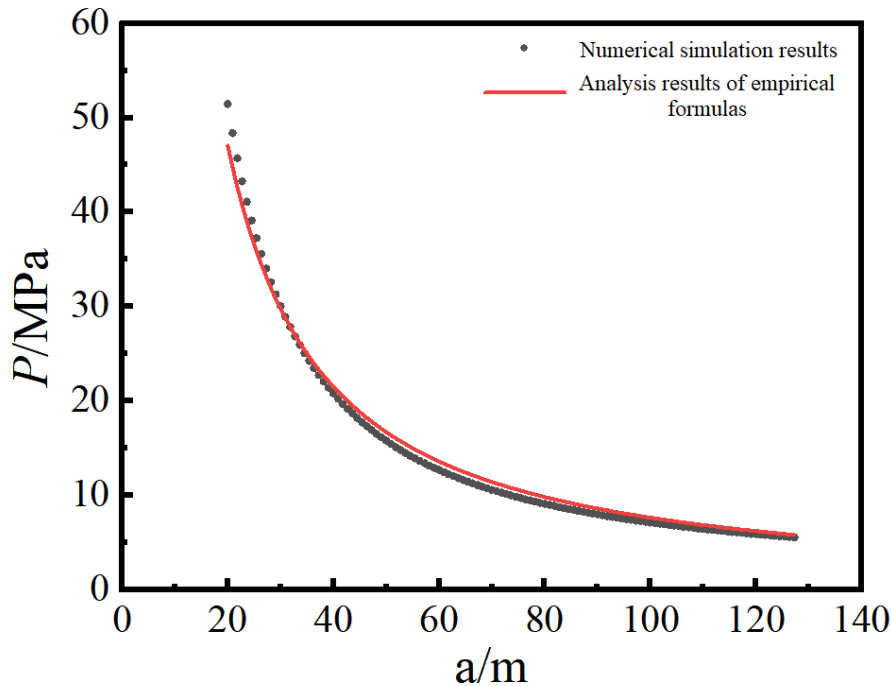


Fig. 6. Comparison of empirical value and calculation of peak pressure at different proportions of detonation distance

3.2. Underwater Continuous Explosion Simulation

Based on the one-dimensional underwater explosion calculation model in Figure 7, a one-dimensional continuous explosion simulation model is established, as shown in Figure 7. A total of 3 charges are set, the charges are detonated at the same interval, the expansion part of the original explosive is refilled with water medium, new charges are set according to the parameters of the original charges, and finally the new charges are filled in the original water. In order to compare the interaction between shock waves at different intervals, three different explosion intervals of 20 ms, 50 ms, and 80 ms were set. To avoid the influence of shock wave reflection on the results, outflow boundary conditions are set.

Figure 8 shows the effect of shock wave propagation with different dosages. It can be seen from Figure 8 that it will increase to the peak pressure instantly after the initiation of the charge, and then the shock wave pressure will rapidly decay to a certain range. The overall trend of the shock wave curve of the post-initiation charge remains unchanged, and it still decreases exponentially. Charge mass has obvious influence on bubble pulsation period, and the smaller the charge mass, the shorter the bubble period.

Figure 9 shows the effect of different explosion intervals of 1 kg charge on shock wave propagation. By observing Figure 9(a), it can be seen that at the 70 m explosion depth, the shock wave pressure of the initiating charge increases when the explosion interval is 20 ms and 80 ms, but the enhancement effect is not obvious; The shock wave pressure of the second charge increased significantly at 50 ms interval, but the peak pressure of the third charge was

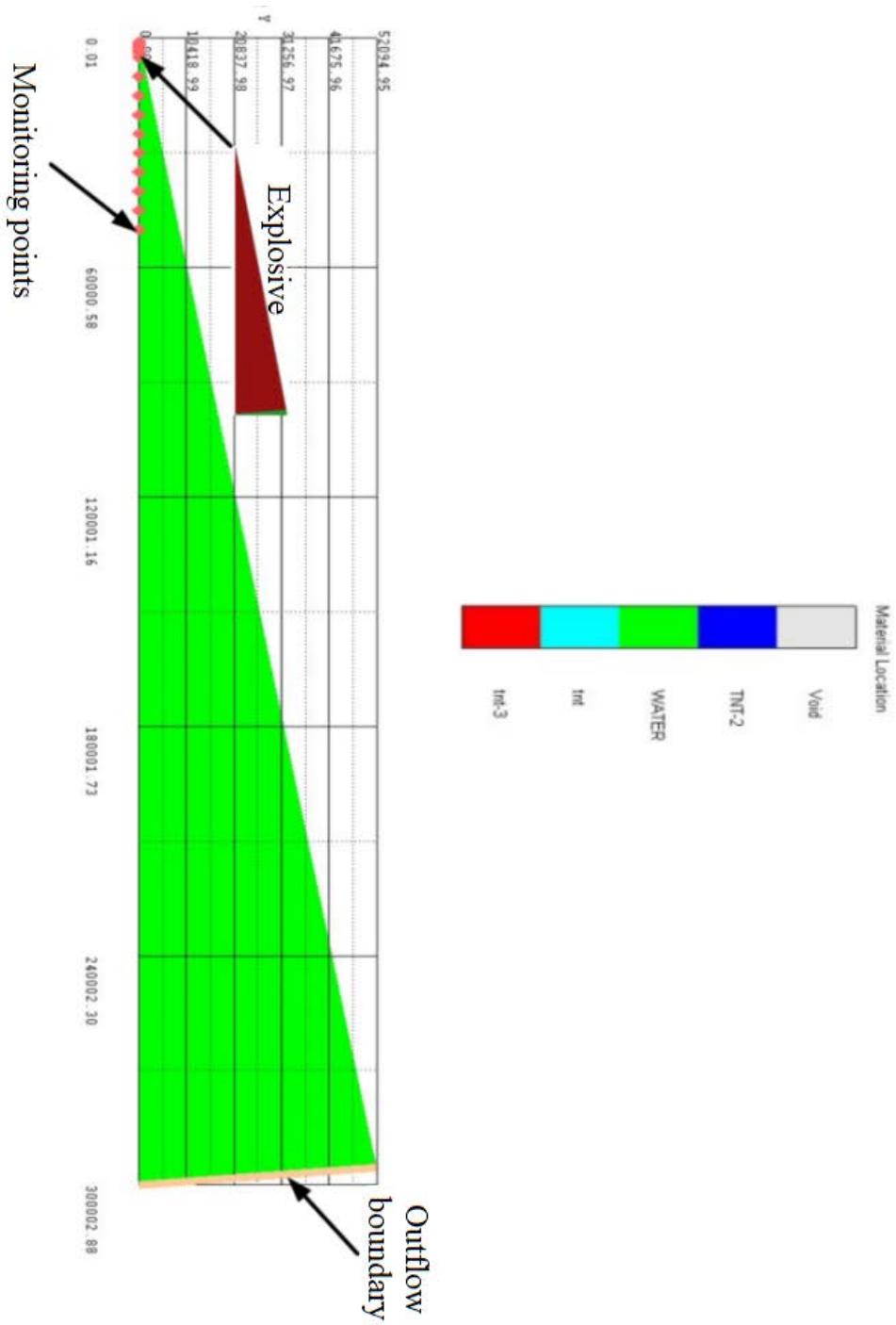
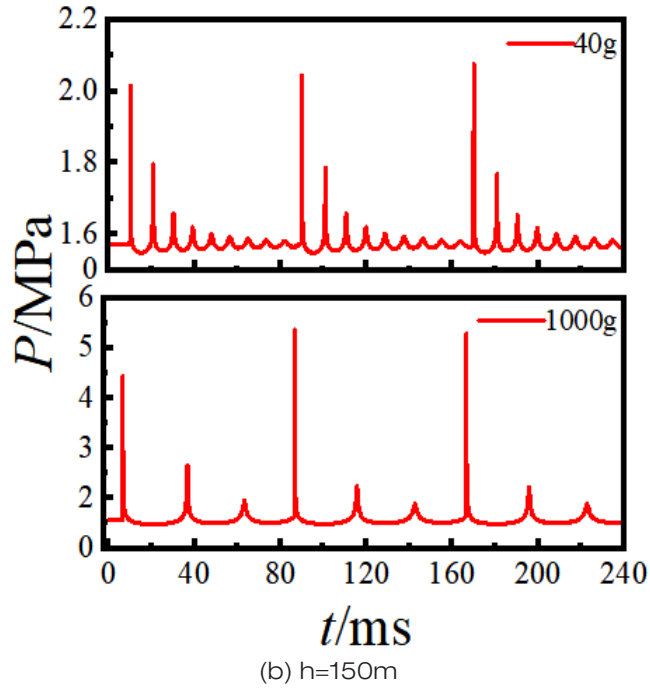
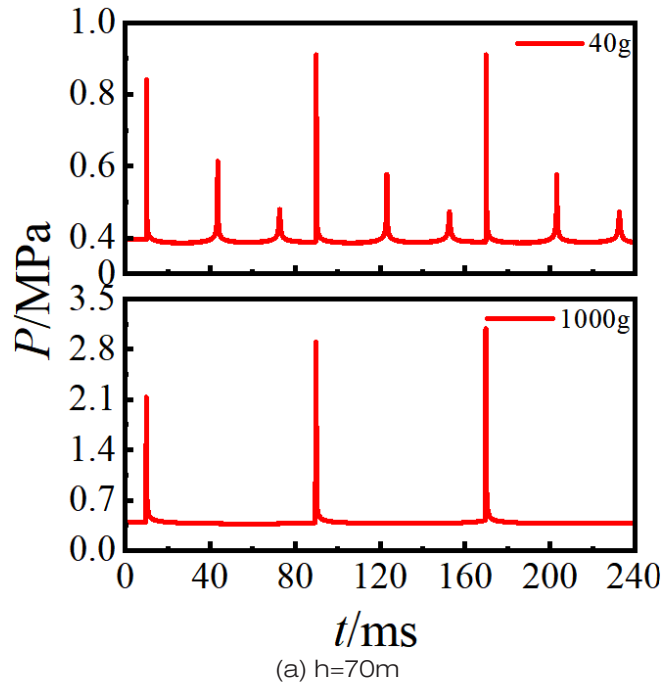


Fig. 7. Simulation calculation model



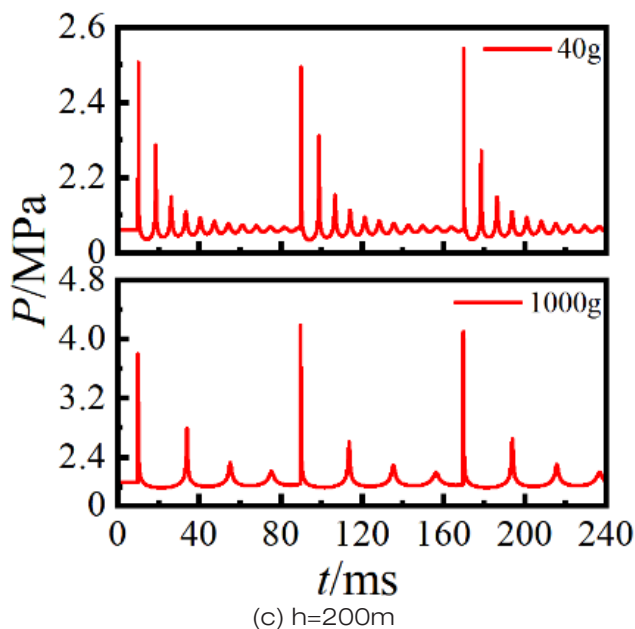


Fig. 8. Effect of shock wave propagation with different dosage

very low. This is due to the influence of bubble pulsation. The initiation time of the third charge is just at the end of the bubble pulsation of the second charge, and the pulsation pressure has been attenuated, so the shock wave pressure is obviously decreased. By observing Figure 9(b), it can be seen that the peak pressure of the post-detonating charge is greater than that of the first charge. The increase of shock wave peak pressure at the interval of 50 ms is due to the initiation time of the post-detonating charge in the rising period of the first bubble pulsation, and the filling explosive will increase the shock wave peak pressure at this time. The peak pressure of the shock wave increases significantly at the interval of 80 ms, which is due to the initiation time of the post-detonating charge just in the rising period of the bubble pulsation of the first charge, which will greatly increase the peak pressure of the shock wave. In summary, due to the different initiation intervals of charge, the state of charge is also different, which has a great influence on the post-detonating charge. Choosing the appropriate explosion interval can effectively improve the underwater explosion power and bring the most obvious interference effect to the target recognition process.

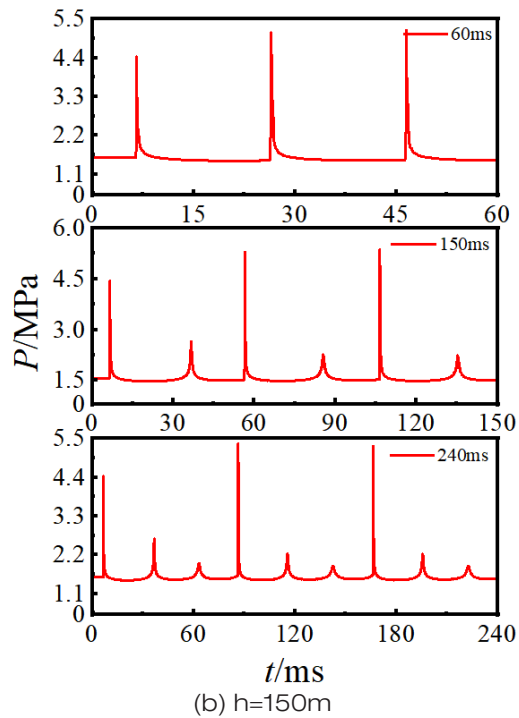
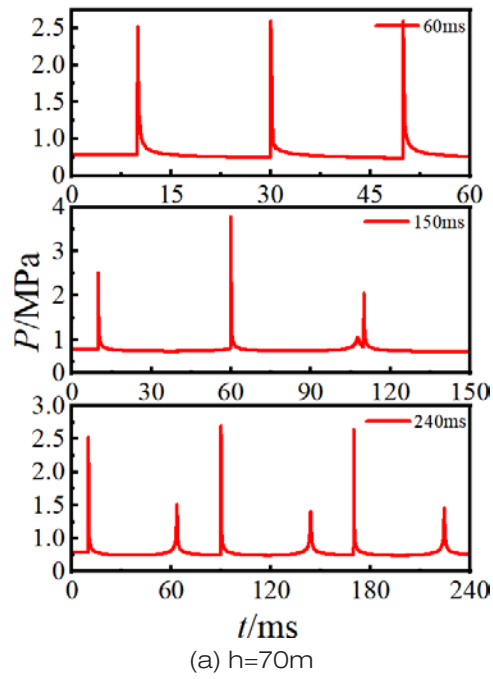


Fig. 9. Effect of different explosion interval time on shock wave propagation

4. ACOUSTIC CHARACTERISTICS OF UNDERWATER CONTINUOUS EXPLOSION

4.1. Sound Velocity Propagation Law

Figure 10 shows the curve of underwater explosion velocity changing with distance. At the explosive charge of 1 kg and the explosion depth of 100 m, 19 monitoring points were evenly set from 0.5 m to 5 m to extract the sound velocity monitored at each monitoring point. In a certain range, with the increase of explosion distance, the shock wave velocity will rapidly decay to the sound velocity in water, and then gradually tend to be flat, and maintain at 1500 m/s. Therefore, it can be inferred that when the shock wave travels far enough, it can be studied as an acoustic signal.

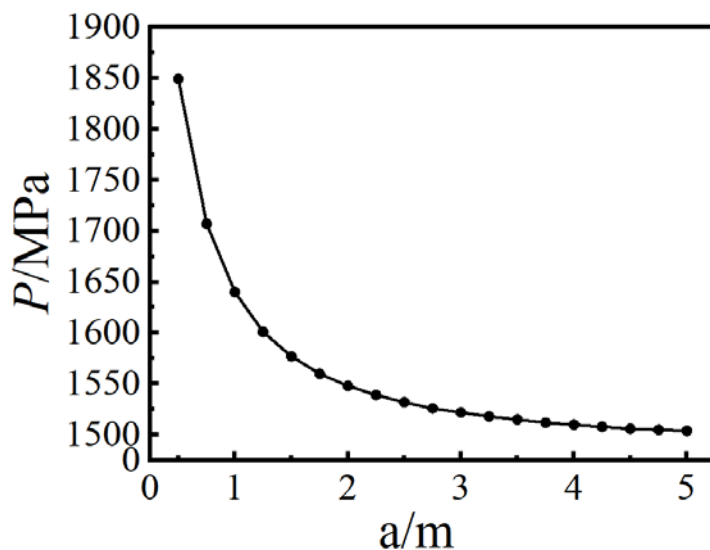
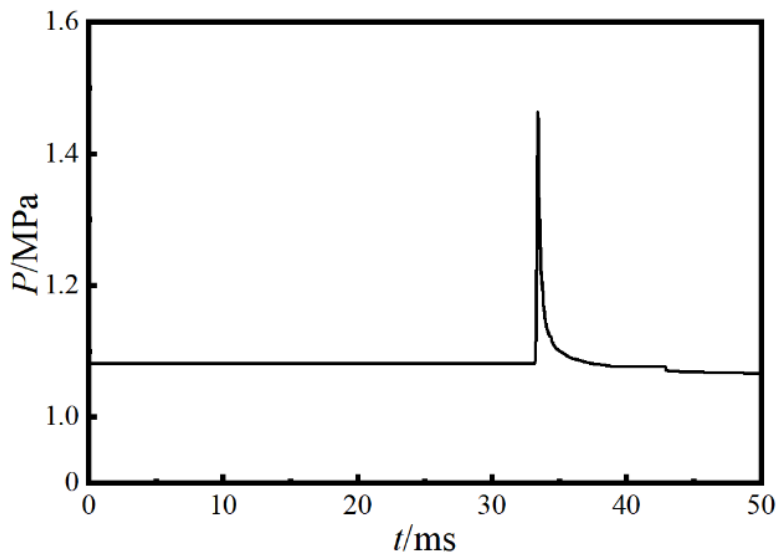


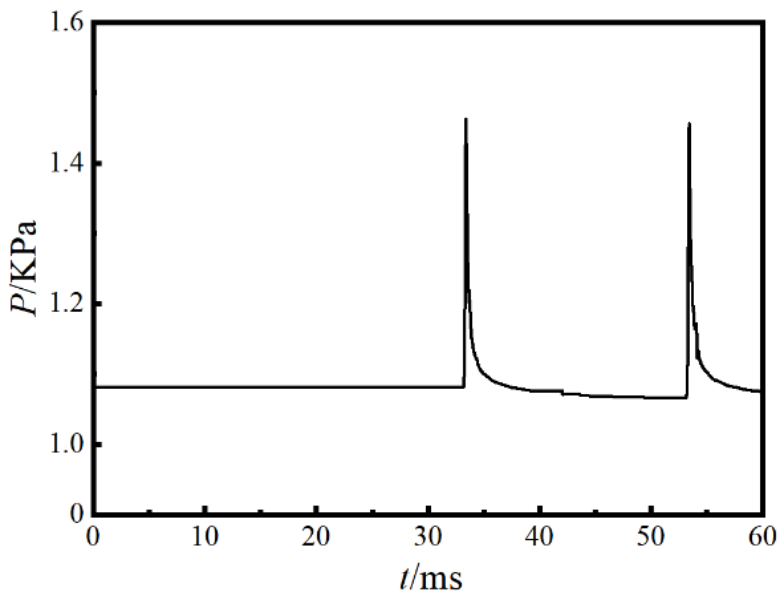
Fig.10. Sound velocity curve of shock waves reaching different explosion distances.

4.2. Duration of Acoustic Signal

The velocity of TNT explosion is 6900 M/s. according to formula (2-1), it can be seen that the duration of pulse pressure generated by a single underwater explosion is very short, so it is impossible to be used as an interference source for underwater acoustic countermeasure. Figure 11 shows the time pressure curves of underwater explosion pulse with 1 kg charge. The explosion position is 100 m away from the water surface, and the monitoring position is 50 m away from the explosion point. When the pulse pressure decays to 90% of the peak value, the pulse pressure width is about 0.19 ms, which also shows that the pressure change is very violent, and the duration is short. The continuous explosion can improve this problem. By properly controlling the underwater explosion time interval of the charge and taking the form of underwater continuous explosion, the continuous acoustic signal of the underwater explosion can be achieved. Fig. 11(b) shows the time pressure curve of continuous explosion pulse with an explosion interval of 20 ms, and the sound duration is effectively extended.



(a) Underwater single-burst



(b) Continuous burst

Fig. 11. Underwater explosion pulse pressure

4.3. Acoustic Pressure and Acoustic Pressure Level

In continuous media, the acoustic pressure is the excess pressure caused by acoustic perturbation. For fluid media, let the static pressure of the volume element in equilibrium state be P_0 and the pressure change to be P when a disturbance is received. The acoustic pressure p is defined as the amount of change in the pressure of the medium:

$$p = P - P_0 \quad (5)$$

Sound pressure is divided into instantaneous sound pressure and effective sound pressure. Instantaneous sound pressure is the pressure obtained by subtracting the static pressure from the instantaneous total pressure at a certain point. Effective sound pressure is the root mean square value of the instantaneous sound pressure at a point over a period of time. In the case of periodic sound pressure, this period of time is taken as the integral multiple of the period. For non-periodic continuous sound waves, this period of time should be long enough so that its length will no longer affect the calculation results. Effective sound pressure P_e satisfy the following relationship [15]:

$$p_e = \frac{p_m}{\sqrt{2}} \quad (6)$$

Sound pressure levels are measured by using a logarithmic scale. The sound pressure level is the ratio of the effective value of the sound pressure somewhere in the sound field to the reference sound pressure taken as a logarithmic measure of the intensity level of the sound and it is defined as:

$$SPL = 20 \times \log(P_e/P_{ref}) \quad (7)$$

where SPL is the sound pressure level at a certain point in the sound field, P_e is the sound pressure at this point, and P_{ref} is the reference sound pressure of the sound field. The reference sound pressure in water is 1×10^{-6} Pa.

Figure 12 shows the corresponding sound pressure levels for 1 kg charge captured at 50 m from the center of the explosion. As can be seen from Figure 12, the sound pressure level from the continuous underwater explosion is high and decays exponentially for each detonation unit; the sound pressure level from bubble pulsation during the underwater explosion cannot be ignored and the first bubble pulsation sound pressure level is only a few decibels smaller than that of the shock wave. By comparing the sound pressure level curves of the three different time intervals in Figure 12(a), it can be seen that as the detonation interval time increases, the sound pressure level at the concave point in the curve gradually decreases, and even smaller than the initial background sound pressure level. The rule of Figure 12(b) is the same as Figure 12(a). Therefore, if the detonation interval time between successive detonation units is reduced, the sound pressure level at the concave point can be increased.

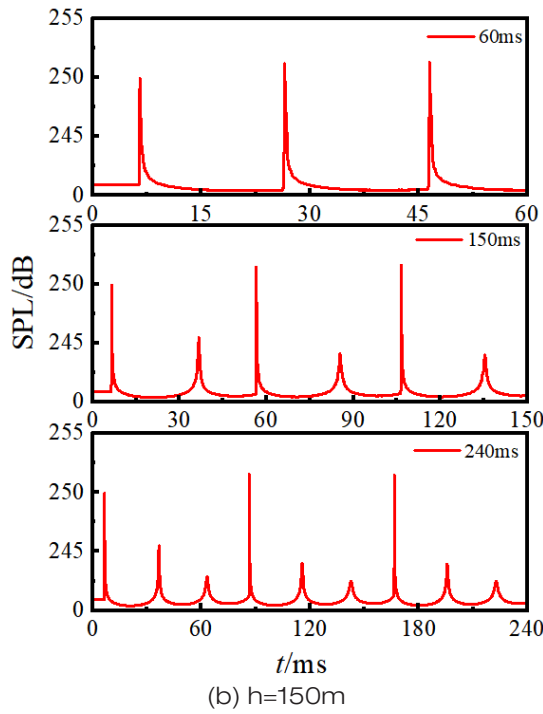
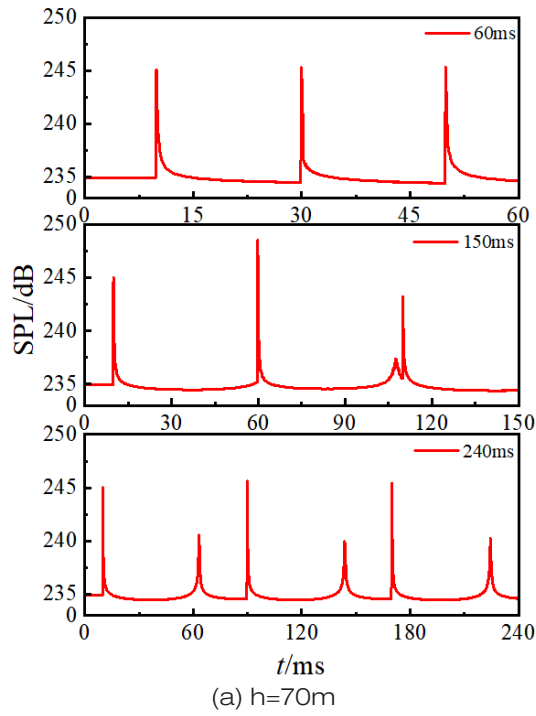
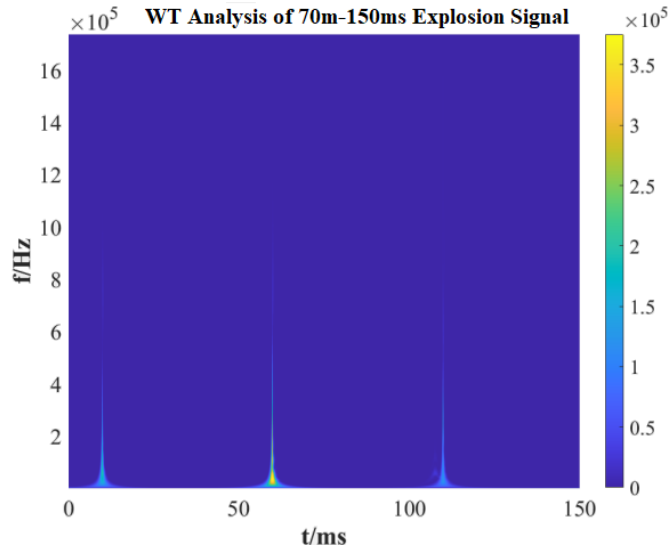


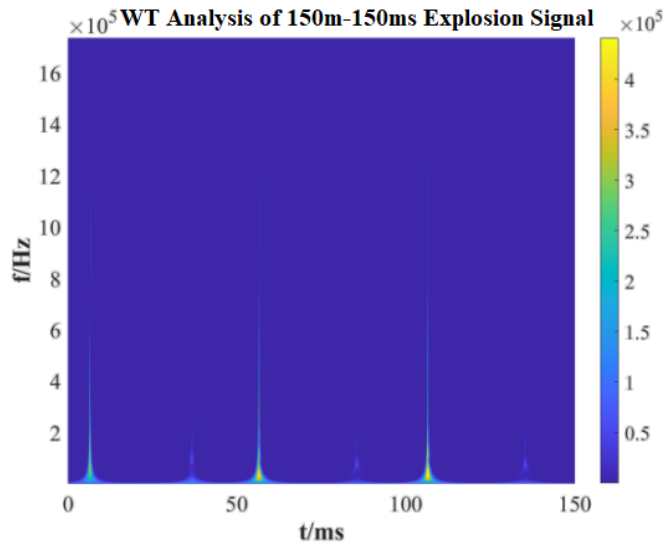
Fig. 12. Different explosion interval sound pressure levels

4.4. Time Frequency Analysis of Explosion Acoustic Signal

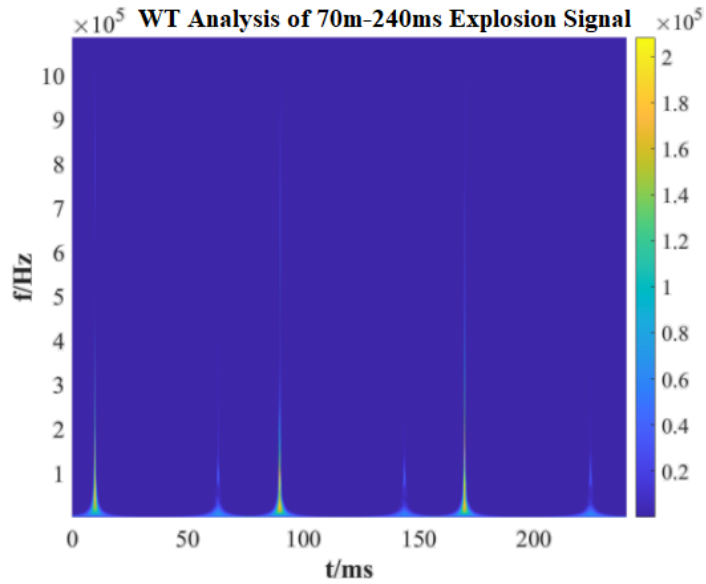
In Figure 12, the original signal reflects its characteristics in the time domain. In order to understand the structure of explosion signal more accurately, wavelet transform is carried out on it, and it is transformed into frequency domain for analysis. Figure 13 shows the time-frequency diagram of the continuous explosion signal. As can be seen from Figure 13, the explosion signal has a wide range of frequency domain distribution and is mainly distributed in the low frequency. The greater the explosion depth is, the wider the frequency distribution range is, and at the same explosion distance, the greater the charge is, the wider the frequency distribution range of the explosion signal is.



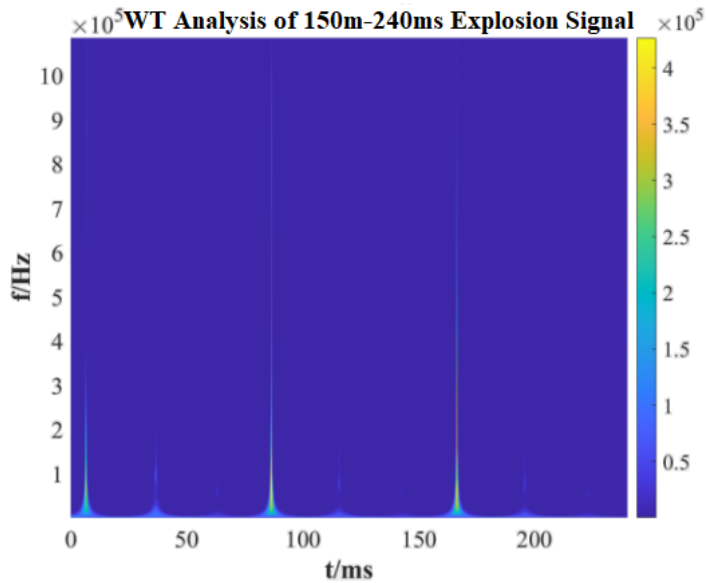
(a) 70 m-150 ms



(b) 150 m-150 ms



(c) 70 m-240 ms



(d) 150 m-240 ms

Fig. 13. Time-frequency diagram of continuous explosion

4.5. Acoustic Power Spectrum

Spectrum (amplitude spectrum and phase spectrum) is one of the methods to describe signal characteristics in the frequency domain, which reflects the distribution of the amplitude and

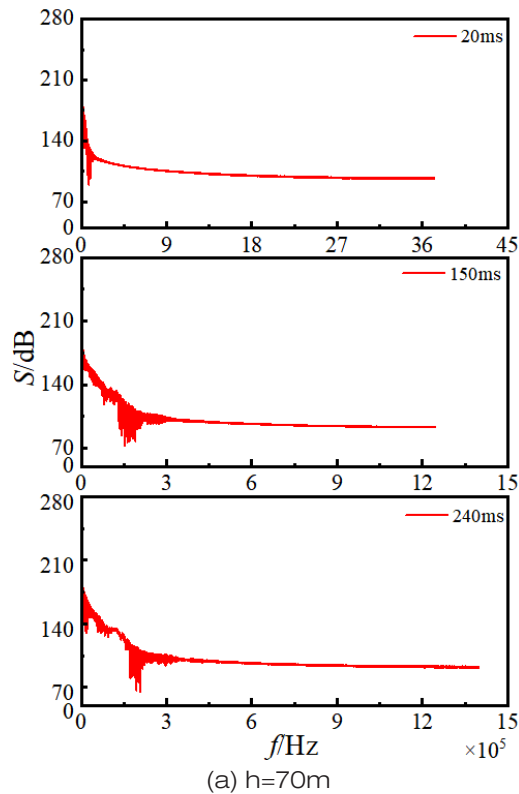
phase of the components contained in the signal with frequency [19]. In addition, energy spectrum or power spectrum can also be used to describe signals. Energy spectrum and power spectrum represent the variation of signal energy or power density with frequency in the frequency domain, which plays an important role in studying the distribution of the signal energy (or power), determining the frequency band occupied by signals and other issues. According to the characteristics of the explosive acoustic, power spectrum is used to describe its frequency domain characteristics. The calculation of power spectrum of random signal is actually to estimate the power spectrum of signal with finite length data, which is called power spectrum or spectral density estimation known as the power spectrum or spectral density estimates. The power spectral density function is:

$$S = \frac{M^2}{N f} \quad (8)$$

where S is the power spectral density, M is the amplitude, N is the number of data, and f is the sampling frequency. The power spectral density unit is converted to dB by the formula:

$$S' = 10 * \lg(S) \quad (9)$$

Figure 14 shows the power spectrum of acoustic signals at different time intervals of underwater continuous explosions. From Figure 14(a), it is found that the energy proportion.



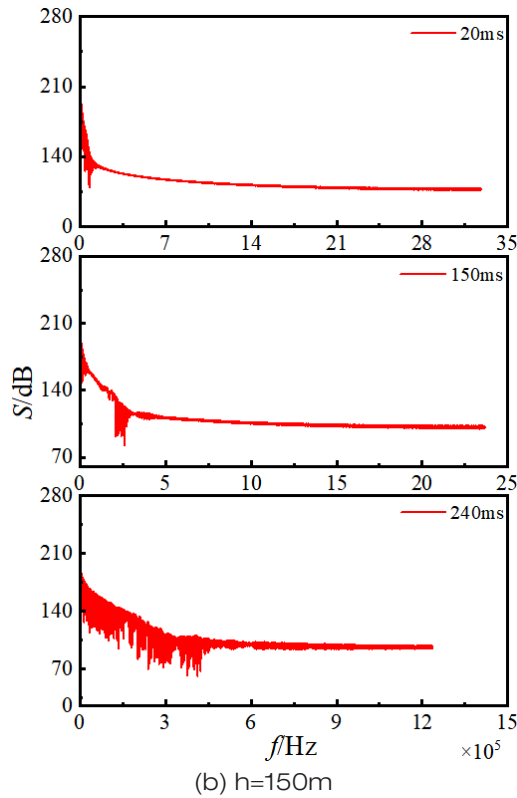


Fig. 14. Power spectrum of acoustic signal at different time intervals

of the low-frequency part increases as the explosion time interval prolongs. After preliminary analysis, it may be the influence of bubble pulsation. Continuing to observe the power spectrum curves of 2 sets of explosion signals with different explosion depths at 80 ms time intervals, the proportion of the low-frequency energy also increases with the increase of explosion depth. This is due to the shortening of the period of bubble pulsation as the explosion depth increases, with the highest number of bubble pulsations generated at 150 m and the highest energy fraction is in its low-frequency portion. Therefore, it can be determined that the dominant factor causing the change in the energy proportion is bubble pulsation, and a concentrated acoustic signal can be obtained by reasonably controlling the detonation interval.

Figure 14 shows the power spectrum of acoustic signals at different explosion depths. The trends of the acoustic signals at different explosion depths are the same. The frequency range of the explosion sound signal is wide enough to cover the operating frequencies of various underwater detection and identification systems. At the explosion depth of 50 m, the acoustic power level decays rapidly from 247 dB to 130 dB in the frequency range 0 to 6×10^5 Hz, and decays slowly above 6×10^5 Hz, oscillating around 120 dB. At a explosion depth of 150 m, the acoustic power level decays rapidly from 257 dB to 140 dB in the frequency range 0- 5.5×10^5 Hz and decays slowly above 5.5×10^5 Hz, remaining in the range of 120 dB. The analysis shows that the explosion depth has a certain influence on the acoustic power level, the greater the explosion depth, the higher the acoustic power level, which finally remains at about

120 dB. In the low-frequency band, the acoustic power level decays rapidly with the increase of frequency, and the acoustic energy is mainly concentrated in the low-frequency part; in the higher-frequency band the acoustic power level decays slowly, and the acoustic energy is lower.

5. CONCLUSION

This paper focuses on the analysis of the acoustic characteristics of underwater continuous explosion acoustic sources by numerical simulation. Firstly, the decay law of the underwater explosion shock wave was studied, the variation of the peak pressure of the shock wave with the depth of the explosion was analyzed, and the accuracy of the numerical simulation was verified by calibrating the empirical formula. After that, the coupling relationship between the underwater continuous explosion shock waves was explored, the shock wave pressure signal was converted into the corresponding sound pressure level, and the regular characteristics of the change of the sound pressure level with the explosion depth were analyzed. Finally, the sound signal was analyzed in frequency domain by time-frequency transformation and power spectrum transformation. The results show that:

- (1) The overall trend of continuous explosion shock wave curve is unchanged and decays exponentially; the state of charge is different with different initiation interval, which has great influence on the post-initiation charge. Choosing a suitable explosion interval time can effectively improve the power of the explosion and has a significant interference effect on the target identification.
- (2) Within a certain range, as the distance of the explosion increases, the shock wave velocity decays rapidly to the speed of sound in water, so it can be considered that when the shock wave travels far enough, it can be treated as an acoustic signal; underwater explosions have strong acoustic power and high sound pressure level, and continuous underwater explosions can effectively increase the sound pressure level.
- (3) The frequency coverage of explosive sound signal is very wide, and the acoustic power level decays rapidly with the increase of frequency in the low frequency range, resulting in high sound energy; in the higher-frequency band acoustic power level decays slowly, and its sound energy is low; bubble pulsation has a great influence on the acoustic power level energy distribution, and the more times of bubble pulsation, the greater the proportion of low-frequency energy.

ACKNOWLEDGMENTS

The authors disclosed receipt of the following financial support for the research, authorship, and/or publication of this article: The authors are grateful for Science research funding project of Liaoning Provincial Department of Education (No. LJKZ0269), and Cultivation and Construction Project of High-level Achievement of Shenyang Ligong University, and Guangxuan Talents of Shenyang Ligong University, and Guangxuan Teams of Shenyang Ligong University.

REFERENCES

- [1] Zhang, C. J., Sun B. W., Mo, Y. X. and Guo, S. M., Analysis of monitoring ability of International Monitoring System hydrophone stations. *Journal of Applied Acoustics*, 2021, 40(4): p. 498-509.
- [2] Guo, R. and Yu, Y. H., Progress and Prospect of the Acoustic Effects of Underwater Explosions. *Journal of Unmanned Undersea Systems*, 2022, 30(3): p. 266-282.
- [3] Sun, Y. X., Tian, J. H., Zhang, Z. F. and Shi, M. B., Experiment and numerical simulation study on the near-field underwater explosion of aluminized explosive. *Journal of Vibration and Shock*, 2020, 39(14): p. 171-178+193.
- [4] Ma, S., Chen, Y. Q., Wang, Z. Q., Wang, J. H., Hu, J., Study on load scaling relationship in centrifuge test of underwater explosion. *China Civil Engineering Journal*, 2021, 54(10): p. 20-29.
- [5] Liu, S. C., Wang, Q. S. and Lou, H. R., Effects of Charge Depth and Air Domain Size on Underwater Explosion. *Journal of Unmanned Undersea Systems*, 2019, 27(6): p. 664-672.
- [6] Meng, L., Huang, R. Y., Wang, J. X., Qin, J. and Liu, L. T., Numerical Simulation of Bubble Pulsation of Small-scaled TNT in Underwater Explosion. *Acta Armamentarii*, 2020, 41(S1): p. 64-71.
- [7] Lu, Q., Pang, L. X., Huang, H. Q., Shen, C., Cao, H. L., Shi, Y. B. and Liu, J., High-g calibration denoising method for high-G MEMS accelerometer based on EMD and wavelet threshold. *Micromachines*, 2019, 10(2): p. 134.
- [8] Li, Y. X. and Wang, L., A novel noise reduction technique for underwater acoustic signals based on complete ensemble empirical mode decomposition with adaptive noise, minimum mean square variance criterion and least mean square adaptive filter. *Defence Technology*, 2020, 16(3): p. 543-554.
- [9] Kim, K. I., Pak, M. I., Chon, B. P. and Ri, C. H., A method for underwater for underwater acoustic signal classification using convolutional neural network combined with discrete wavelet transform. *International Journal of Wavelets, Multiresolution and Information Processing*, 2021, 19(4): p. 2050092.
- [10] Du, Z. P., Wang, Y., Yang, Y., Hua, H. X. and Shi, S. H., Curve Fit Method for Naval Underwater Explosion Shock Signal and Its Application. *Journal of Vibration and Shock*, 2010, 29(3): p. 182-184+213.
- [11] Wei, Z. X., Ju, Y. and Song, M., A method of underwater acoustic signal classification based on deep neural network. 2018 5th International Conference on Information Science and Control Engineering (ICISCE), Zhengzhou, China, IEEE, 2018, p. 46-50.
- [12] Weston, D. E., Underwater Explosions as Acoustic Sources. *Proceedings of the Physical Society*, 1960, 76(2): p. 233-249.
- [13] Arons, A. B., Underwater Explosion Shock Wave Parameters at Large Distances from the Charge. *The Journal of the Acoustical Society of America*, 1954, 26(3): p. 343-346.
- [14] Arons, A. B., Secondary Pressure Pulses Due to Gas Globe Oscillation in Underwater Explosions. II. Selection of Adiabatic Parameters in the Theory of Oscillation. *Journal of the Acoustical Society of America*, 1948, 20(3): p. 277-282.

- [15] Liu, L., Guo, R. and Liu, R. Z., Identification and time-frequency analysis of direct components from the underwater explosion in the shallow water. *Journal of Terahertz Science and Electronic Information Technology*, 2018, 16(3): p. 501-509.
- [16] Wu, C., Liao, S. S., Li, H. X., Zhang, X. R., Zhang, Y. X. and Shi, J. Z., An Investigation and Analysis on the Acoustic Characteristics of Three Types of Explosive Charges by Underwater Explosion. *Transactions of Beijing institute of Technology*, 2009, 29(1): p.1-4.
- [17] Fan, Z. Q., Ma, H. H., Shen, Z. W. and Jiang, Y. G., Acoustic characteristics of underwater continuous pulse shock wave. *Explosion and Shock Waves*, 2013, 33(5): p. 501-506.
- [18] Sheng, Z. X., *Research on Underwater Sequential Explosions and Acoustic Characteristics*. Nanjing University of Science and Technology, 2013.
- [19] Jiang, G., Cao, L., Time-frequency Characteristics of Underwater Explosion Signal Based on Hilbert-huang Transform. *Ship Electronic Engineering*, 2020, 40(9): p. 153-156.